Variations of the Diferric Exchange Coupling in the R2 Subunit of Ribonucleotide Reductase from Four Species as Determined by Saturation−Recovery EPR Spectroscopy

C. Galli,[†] Mohamed Atta,[‡] K. Kristoffer Andersson,*[,‡,§] Astrid Gräslund,*[,‡] and Gary W. Brudvig*[,†]

Contribution from the Department of Chemistry, Yale University, New Haven, Connecticut 06511, and Department of Biophysics, Stockholm University, Stockholm, Sweden S-106 91

Received August 18, 1994[⊗]

Abstract: The R2 subunit of ribonucleotide reductase (RNR) contains a stable tyrosine radical coupled to an adjacent diferric center. The spin−lattice relaxation rate of the tyrosine radical is greatly enhanced above 20 K due to the paramagnetic excited states of the diferric center. By using saturation−recovery electron paramagnetic resonance (EPR) spectroscopy, we have examined the spin−lattice relaxation dynamics of the tyrosine radical in R2 proteins from mouse, herpes simplex virus type 1, *Escherichia coli*, and *Salmonella thyphimurium* within the temperature range of 4−70 K. These measurements yield the diferric exchange coupling as well as the radical−metal coupling, which contains both exchange and dipolar components. In all four species, the ground state of the diferric center is diamagnetic, indicating that the two Fe(III)s are antiferromagnetically exchange-coupled. The diferric exchange interaction ($H = -2JS_1S_2$) is found to vary from $J = -66$ cm^{-1} (herpes simplex virus type 1) to $J = -92$ cm^{-1} (*E. coli*). Measurements on samples in deuterated buffer suggest that the variation of the diferric exchange coupling among species may result from differences in hydrogen bonding to the μ-oxo bridge between the ferric ions. An interpretation of the observed spin−lattice relaxation channels of the tyrosine radicals on the basis of the spectroscopic data, as well as the published three-dimensional structure of the R2 protein from *E. coli*, is offered.

Introduction

Ribonucleotide reductase (RNR) catalyzes the reduction of ribonucleotides to their corresponding deoxy form and is found in a wide range of species including eukaryotes, bacteria, bacteriophages, and eukaryotic viruses. Due to the central role played by RNR in cellular reproduction, the mechanism and regulation of RNR has been an active research area. The RNR holoenzyme in its active form, $\alpha_2\beta_2$, consists of two proteins: R1 and R2. The larger subunit, R1, provides substrate binding sites for the ribonucleoside diphosphates and contains the redox-active dithiol groups for the reduction of the ribonucleotide groups.[1] The crystal structure of the R2 protein from *Escherichia coli* has recently been determined at 2.2 Å resolution.[2] Each polypeptide chain of the R2 homodimer contains a dinuclear metallic center consisting of two nonheme Fe(III) ions and a stable tyrosine radical, Tyr 122; the centers of these two moieties are separated by 8.3 Å. Both the tyrosine radical and the diferric center are required for enzymatic activity. The two Fe(III) ions are linked by a μ-oxo-μ-carboxylato bridge that mediates strong antiferromagnetic exchange coupling between the Fe(III) ions; the exchange coupling between the Fe(III) ions, J_{ex}(Fe−Fe), is approximately −90 cm^{-1} in the R2 protein from *E. coli* ($H = -2JS_1S_2$).[3] The R2 protein is structurally related to other proteins[4] containing oxygen-bridged metallic centers such as hemerythrin,[5] methane monooxygenase,[6] purple acid phosphatases,[7] and hemocyanin.[8] As intact metallic centers are required for protein activity, elucidation of the exchange interactions present in these metalloproteins is required for a detailed description of the interplay between the electronic structure of the metallic center and the dynamics of the protein activity.

The spin−lattice relaxation of the tyrosine radical in the R2 protein is greatly enhanced above 20 K due to the paramagnetic

[†] Yale University.

[‡] Stockholm University.

[§] Current address: Department of Biochemistry, University of Oslo, Oslo, Norway N-0316.

[⊗] Abstract published in *Advance ACS Abstracts*, December 15, 1994.

(1) (a) Reichard, P.; Ehrenberg, A. *Science* **1983**, *221*, 514−519. (b) Sjöberg, B.-M.; Gräslund, A. *Adv. Inorg. Biochem.* **1983**, *5*, 87−110. (c) Stubbe, J. *Adv. Enzymol.* **1990**, *63*, 349−419. (d) Fontecave, M.; Nordlund, P.; Eklund, H.; Reichard, P. *Adv. Enzymol.* **1992**, *65*, 83−147. (e) Reichard, P. *Science* **1993**, *260*, 1773−1777.

(2) (a) Nordlund, P.; Sjöberg, B.-M.; Eklund, H. *Nature* **1990**, *345*, 593−598. (b) Nordlund, P.; Eklund, H. *J. Mol. Biol.* **1993**, *232*, 123−164. (c) The crystallographic structure was determined for the radical-free form of the R2 protein.

(3) (a) Petersson, L.; Gräslund, A.; Ehrenberg, A.; Sjöberg, B.-M.; Reichard, P. *J. Biol. Chem.* **1980**, *255*, 6706−6712. (b) Hirsh, D. J.; Beck, W. F.; Lynch, J. B.; Que, L., Jr.; Brudvig, G. W. *J. Am. Chem. Soc.* **1992**, *114*, 7475−7481. (c) Atta, M.; Scheer, C.; Fries, P. H.; Fontecave, M.; Latour, J.-M. *Angew. Chem., Int. Ed. Engl.* **1992**, *31*, 1513−1515.

(4) (a) Sanders-Loehr, J. In *Iron Carriers and Iron Proteins*; Loehr, T. M., Ed.; VCH Press: New York, 1989; pp 373−466. (b) Vincent, J. B.; Olivier-Lilley, G. C.; Averill, B. A. *Chem. Rev.* **1990**, *90*, 1447−1467. (c) Que, L., Jr.; True, A. E. In *Progress in Inorganic Chemistry: Bioinorganic Chemistry;* Lippard, S. J., Ed.; John Wiley & Sons: New York, 1990; Vol. 38, pp 97−200. (d) Solomon, E. I.; Zhang, Y. *Acc. Chem. Res.* **1992**, *25*, 343−352. (e) Lippard, S. J. *Angew. Chem., Int. Ed. Engl.* **1988**, *27*, 344−361. (f) Kurtz, D. M., Jr. *Chem. Rev.* **1990**, *90*, 585−606.

(5) (a) Scheriff, S.; Hendrickson, W. A.; Smith, J. L. *J. Mol. Biol.* **1987**, *197*, 273−296. (b) Holms, M. A.; Stenkamp, R. E. *J. Mol. Biol.* **1991**, *220*, 723−737. (c) Reem, R. C.; McCormick, J. M.; Richardson, D. E.; Devlin, F. J.; Stephens, P. J.; Musselman, R. L.; Solomon, E. I. *J. Am. Chem. Soc.* **1989**, *111*, 4688−4704. (d) Muhoberac, B. B.; Wharton, D. C.; Babcock, L. M.; Harrington, P. C.; Wilkins, R. G. *Biochim. Biophys. Acta.* **1980**, *626*, 337−345. (e) Pearce, L. L.; Kurtz, D. M., Jr.; Xia, Y.-M.; Debrunner, P. G. *J. Am. Chem. Soc.* **1987**, *109*, 7286−7293. (f) McCormick, J. M.; Reem, R. C.; Solomon, E. I. *J. Am. Chem. Soc.* **1991**, *113*, 9066−9079.

(6) (a) Rosenzweig, A. C.; Frederick, C. A.; Lippard, S. J.; Nordlund, P. *Nature* **1993**, *366*, 537−543. (b) DeWitt, J. G.; Bensten, J. G.; Rosenzweig, A. C.; Hedman, B.; Green, J.; Pilkington, S.; Papaefthymiou, G. C.; Dalton, H.; Hodgson, K. O.; Lippard, S. J. *J. Am. Chem. Soc.* **1991**, *113*, 9219−9235. (c) Andersson, K. K.; Elgren, T. E.; Que, L., Jr.; Lipscomb, J. D. *J. Am. Chem. Soc.* **1992**, *114*, 8711−8713. (d) Lipscomb, J. D. *Annu. Rev. Microbiol.* **1994**, *48*, 371−399.

0002-7863/95/1517-0740$09.00/0

excited states of the diferric center.[3b,9] Two temperature regimes exist. At low temperature, the diferric center is in its ground state ($S = 0$), and the tyrosine radical exhibits single-exponential spin–lattice relaxation kinetics characteristic of a noninteracting spin. As the temperature is increased, the paramagnetic excited states of the diferric center are thermally populated and the spin–lattice relaxation of the tyrosine radical is greatly enhanced and becomes non-single-exponential. We have shown in earlier work that an analysis of the spin–lattice relaxation kinetics in the high-temperature regime allows one to determine the diferric exchange coupling as well as the radical–metal coupling, which contains both exchange and dipolar components.[3b]

This study presents the results of a saturation–recovery electron paramagnetic resonance (EPR) spectroscopic examination of the spin–lattice relaxation of the tyrosine radical in the R2 protein from four species: *E. coli*, herpes simplex virus type 1 (HSV1), mouse, and *Salmonella thyphimurium*. A previous saturation–recovery EPR investigation of the tyrosine radical in the R2 protein from *E. coli* revealed single-exponential recoveries at low temperatures ($T < 15$ K) indicative of the intrinsic spin–lattice relaxation.[3b] The analysis of the non-exponential recoveries observed at higher temperatures allowed for a determination of the diferric exchange coupling, -94 ± 7 cm^{-1}. Although progressive microwave power saturation studies of the tyrosine radicals in the R2 proteins from HSV1 and mouse have shown that their spin–lattice relaxation rates are about 2 orders of magnitude faster at 30 K than in the *E. coli* protein,[9,10] the source of this rapid relaxation was not known. We have determined a significant variation in the diferric exchange coupling among the species, which can account for this difference in relaxation rate and may relate to variations in the chemical reactivity of the site.

Experimental Section

Recombinant mouse and HSV1 R2 proteins were prepared as previously reported.[10] Regeneration of the iron–tyrosine radical site in the mouse and HSV1 R2 was performed by a reaction with ferrous iron and O_2 as previously described.[10] The *S. thyphimurium* R2 protein was prepared as previously described.[11] The *E. coli* R2 protein was purified as previously reported.[12] The radical and iron content per protein were also as previously reported, although 20% more radical per protein was occasionally observed. Protein concentrations were determined colorimetrically by the Bradford method using bovine serum albumin as a standard and from the absorbance difference at 280–310 nm using molar extinction coefficients of 124 000 M^{-1} cm^{-1}, 120 000 M^{-1} cm^{-1}, and 104 000 M^{-1} cm^{-1} for the R2 proteins from mouse, *E. coli*, and HSV1, respectively.[10,12]

Samples of active R2 proteins from mouse and HSV1 reconstituted in deuterated buffer were prepared by first exchanging the apoproteins into 99.5% D_2O by centrifuging apoprotein R2 using a Penefsky centrifuge column[13,14] equilibrated with 100 mM Tris-DCl (pH 7.6) containing 100 mM KCl (pD was corrected for the deuterium isotope effect). Then the active radical-containing R2 protein was prepared by a reaction with ferrous iron and O_2 as described above but using the same D_2O buffers.

All R2 RNR samples used in this study were examined with respect to microwave power saturation by continuous wave EPR in the range from 25 to 77 K. The *E. coli*, mouse, and HSV1 R2 protein samples showed the same behavior as reported by Sahlin et al.[9] and Mann et al.[10] However, the tyrosine radical in *S. thyphimurium* R2 was much more easily saturated than the other three R2 proteins, and, at 25 K, it had a power at half saturation, $P_{1/2}$, very close to that observed for a free tyrosine radical without magnetic interaction with another paramagnetic center (see Sahlin et al.[9] for measurements on a non-protein-bound tyrosine radical). After reconstitution in D_2O, the mouse R2 protein showed a small decrease in $P_{1/2}$, whereas the HSV1 R2 protein showed no change in $P_{1/2}$.

Twenty-percent (v/v) glycerol was added to each sample in order to form a good glass upon freezing. This fraction of glycerol has been shown to preserve the native protein form.[3b] The resulting solution was centrifuged, and the supernatant was examined for optical clarity and subsequently stored in liquid nitrogen. The R2 protein samples used for the EPR measurements contained 100–700 μM radical concentration.

The home-built X-band EPR spectrometer employed and the methods for measuring both continuous wave and saturation–recovery EPR have been previously described.[15] The saturation–recovery EPR data were obtained by tuning the external magnetic field to the low-field zero crossing of the first-derivative absorption spectra (shown by arrows in Figure 1). The saturation–recovery transients were obtained with direct detection (without magnetic field or microwave frequency modulation) by using an observation microwave power of ~0.075–75 μW. As high observation microwave powers are known to distort the spin–lattice relaxation data,[15] minimum observation powers were employed. A microwave pulse of ~0.2–20 mW excited the spin population. Care was taken to ensure that the observed relaxation dynamics displayed no dependence on the power of the excitation pulse. The number of transients averaged to achieve the desired signal-to-noise ratio varied from approximately 10^2 to 10^5.

Theory

Three processes have been found to contribute to the spin–lattice relaxation of the tyrosine radical in the R2 subunit of *E. coli* RNR: (i) the intrinsic relaxation rate of the tyrosine radical in the absence of the diferric center, k_{1i}, (ii) the relaxation rate due to the exchange interaction between the tyrosine radical and the diferric center, k_{1ex}, and (iii) the relaxation rate due to the dipole–dipole interaction between the tyrosine radical and the diferric center, k_{1d}.[3b,9] Two temperature regimes were distinguished. In the low-temperature regime (below ~20 K), where only the diamagnetic ground state of the diferric center is populated, the spin–lattice relaxation of the tyrosine radical is determined by its intrinsic relaxation rate. The magnitude of k_{1i} depends on processes by which spin quanta are converted to lattice phonons of the matrix surrounding the tyrosine radical. Low-temperature saturation–recovery EPR data of the tyrosine radical in the R2 protein, thus, report on spin–phonon coupling mechanisms. In the high-temperature regime, the paramagnetic excited states of the diferric center are thermally populated, and the spin–lattice relaxation of the tyrosine radical is dominated by exchange and dipole–dipole interaction mechanisms. Therefore, the high-temperature saturation–recovery EPR data of the tyrosine radical in the R2 protein provide information on the distance and exchange interaction between the tyrosine radical

(7) (a) Antanaitis, B. C.; Aisen, P. *J. Biol. Chem.* **1982**, *257*, 5330–5332. (b) Antanaitis, B. C.; Aisen, P.; Lilienthal, H. R. *J. Biol. Chem.* **1983**, *258*, 3166–3172. (c) Averill, B. A.; Davis, J. C.; Burman, S.; Zirino, T.; Sanders-Loehr, J.; Loehr, T. M.; Sage, J. T.; Debrunner, P. G. *J. Am. Chem. Soc.* **1987**, *109*, 3760–3767. (d) Doi, K.; Antanaitis, B. C.; Aisen, P. *Struct. Bonding (Berlin)* **1988**, *70*, 1–26. (e) Vincent, J. B.; Averill, B. A.; *FASEB J.* **1990**, *4*, 3009–3014. (f) Scarrow, R. C.; Pyrz, J. W.; Que, L., Jr. *J. Am. Chem. Soc.* **1990**, *112*, 657–665. (g) David, S. S.; Que, L., Jr. *J. Am. Chem. Soc.* **1990**, *112*, 6455–6463. (h) True, A. E.; Scarrow, R. C.; Randall, C. R.; Holz, R. C.; Que, L., Jr. *J. Am. Chem. Soc.* **1993**, *115*, 4246–4255.

(8) Préaux, G.; Gielens, C. In *Copper Proteins and Copper Enzymes*; Lontie, R., Ed.; CRC Press, Inc.: Boca Raton, FL, 1984; Vol. II, pp 159–205.

(9) Sahlin, M.; Petersson, L.; Gräslund, A.; Ehrenberg, A.; Sjöberg, B.-M.; Thelander, L. *Biochemistry* **1987**, *26*, 5541–5548.

(10) Mann, G. J.; Gräslund, A.; Ochiai, E.-I.; Ingemarson, R.; Thelander, L. *Biochemistry* **1991**, *30*, 1939–1947.

(11) (a) Jordan, A.; Gilbert, I.; Barbé, J. *J. Bacteriol.* **1994**, *176*, 3420–3427. (b) Jordan, A.; Pontis, E.; Atta, M.; Krook, M.; Gilbert, I.; Barbé, J.; Reichard, P. *Proc. Natl. Acad. Sci. U.S.A.* **1994**, in press.

(12) Sjöberg, B.-M.; Hahne, S.; Karlsson, M.; Jörnvall, H.; Göransson, M.; Uhlin, B. E. *J. Biol. Chem.* **1986**, *261*, 5658–5662.

(13) Penefsky, H. S. *Methods Enzymol.* **1979**, *56*, 527–530.

(14) Allard, P.; Kuprin, S.; Shen, B.; Ehrenberg, A. *Eur. J. Biochem.* **1992**, *208*, 635–642.

(15) Beck, W. F.; Innes, J. B.; Lynch, J. B.; Brudvig, G. W. *J. Magn. Reson.* **1991**, *91*, 12–29.

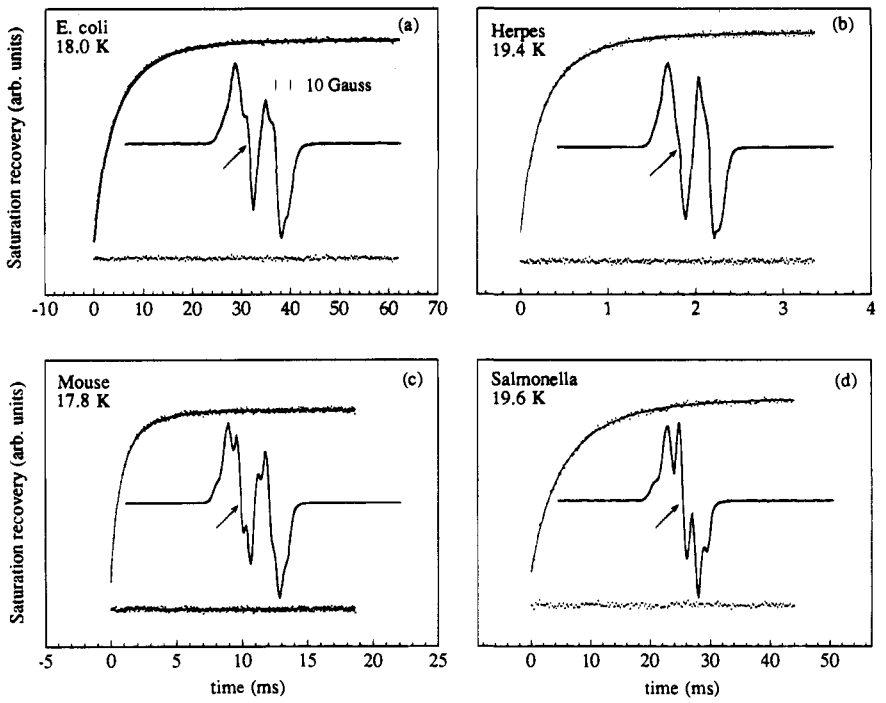

Figure 1. Saturation–recovery EPR transients taken at 18–19 K of the tyrosine radicals in the R2 proteins from (a) *E. coli*, (b) HSV1, (c) mouse, and (d) *Salmonella*. The experimental temperatures are given in the figure. The dots are the data, and the superimposed solid line is the least-squares fit of eq 1. The residuals from the fit are shown along the bottom of each transient. The figure insets show the field-swept EPR spectra of the tyrosine radicals, with an arrow indicating the magnetic-field setting used for the saturation–recovery EPR experiments.

and the diferric center. In addition, the temperature dependence of the relaxation enhancement depends on the magnetic moment of the diferric center, which reflects the exchange interaction between the two Fe(III) ions.

The observed saturation–recovery transient from a randomly ordered sample is the weighted sum of these three relaxation processes. The transient signal, $I(t)$, is given by integrating over all orientations, θ, between the interspin vector and the static magnetic field:

$$I(t) = 1 - N\int_0^{\pi} \sin\theta(e^{-\{k_{1\text{scalar}} + k_{1\theta}\}t})\, d\theta \qquad (1)$$

where N is a normalization constant, $k_{1\text{scalar}}$ is the relaxation rate arising from isotropic processes, and $k_{1\theta}$ is the relaxation rate arising from the orientation-dependent dipole–dipole interaction.[16] This analysis is applicable when the anisotropic contribution to the **g** or hyperfine tensor is appreciably less than the isotropic contribution,[16] as is the case for the *E. coli* R2 protein.[3b,17] (For transitions with large **g** or hyperfine anisotropy, it may be possible to excite subsets of the molecular ensemble by varying the external magnetic field. However, in the present case of the R2 RNR tyrosine radicals, no effect on the recovery kinetics was observed when the external magnetic field was stepped through the EPR spectrum.)

The isotropic term contains contributions from both the intrinsic relaxation rate and the exchange interaction (eq 2). The

$$k_{1\text{scalar}} = k_{1\text{i}} + k_{1\text{ex}} \qquad (2)$$

rate constant, $k_{1\text{ex}}$, for the spin–lattice relaxation due to isotropic exchange between the diferric center, Fe_2, and the tyrosine radical, Y, is given by eq 3

$$k_{1\text{ex}} = \frac{2(J_{\text{ex}}(Fe_2\text{–}Y))^2\mu_{\text{eff}}^2}{3g_f^2\beta^2}\,\frac{1}{\omega_s^2\left(1 - \frac{g_f}{g_s}\right)^2 T_{2f}} \qquad (3)$$

where $J_{\text{ex}}(Fe_2\text{–}Y)$ is the exchange coupling between the diferric center and the tyrosine radical, μ_{eff} is the magnetic moment of the diferric center, g_f and g_s are the g factors of the diferric center and tyrosine radical, respectively, β is the Bohr magneton, ω_s is the Larmor frequency of the tyrosine radical, and T_{2f} is the electron spin–spin correlation time of the diferric center.

The orientation-dependent dipolar–dipole relaxation has been shown, in the case of the tyrosine radical in the *E. coli* R2 protein,[3b] to arise from the "B term" of the dipolar alphabet in the limit where $(\omega_s - \omega_f)^2 \ll \omega_s^2$ and $(\omega_s - \omega_f)^2 T_{2f}^2 \ll 1$ as in eqs 4 and 5,

$$k_{1\theta} = k_{1\text{d}}(1 - 3\cos^2\theta)^2 \qquad (4)$$

$$k_{1\text{d}} = \frac{\gamma_s^2\mu_{\text{eff}}^2}{6r^6}\,\frac{1}{\omega_s^2\left(1 - \frac{g_f}{g_s}\right)^2 T_{2f}} \qquad (5)$$

where γ_s is the magnetogyric ratio of the tyrosine radical, r is the length of the interspin vector, and the remaining terms are defined above.

The saturation–recovery EPR transient of the tyrosine radical in the R2 protein changes both qualitatively and quantitatively as the temperature is raised. In the low-temperature regime, where the spin–lattice relaxation rate is given by $k_{1\text{i}}$, the saturation–recovery EPR transient is single-exponential. In the high-temperature regime, the exchange and dipole–dipole interactions not only lead to markedly faster relaxation rates, but the orientation dependence of the dipole–dipole interaction produces non-single-exponential relaxation kinetics. By fitting

(16) (a) Hirsh, D. J.; Beck, W. F.; Innes, J. B.; Brudvig, G. W. *Biochemistry* **1992**, *31*, 532–541. (b) Hirsh, D. J.; Brudvig, G. W. *J. Phys. Chem.* **1993**, *97*, 13216–13222.

(17) (a) Sjöberg, B.-M.; Reichard, P.; Gräslund, A.; Ehrenberg, A. *J. Biol. Chem.* **1978**, *253*, 6863–6865. (b) Bender, C. J.; Sahlin, M.; Babcock, G. T.; Barry, B. A.; Chandrashekar, T. K.; Salowe, S. P.; Stubbe, J.; Lindström, B.; Petersson, L.; Ehrenberg, A.; Sjöberg, B.-M. *J. Am. Chem. Soc.* **1989**, *111*, 8076–8083.

eq 1 to the experimental saturation–recovery EPR data, we can extract both $k_{1\text{scalar}}$ and $k_{1\theta}$.[3b]

As previously shown,[3b] the only temperature-dependent factor in eqs 3 and 5 is μ_{eff}^2. Thus, $k_{1\text{scalar}}$ and $k_{1\theta}$ are expected to have the same temperature dependence, and their temperature dependence will directly reflect the exchange coupling between the two Fe(III) ions. At very low temperatures, $k_BT \ll J_{ex}$(Fe–Fe), $\mu_{\text{eff}} \sim 0$. However, at higher temperatures, the excited triplet and higher-energy spin states of the diferric center are thermally populated. The magnetic moment of the diferric center, μ_{eff}, is a function of the population in the excited spin states. Equation 6 gives μ_{eff} as a function of temperature in units of Bohr magnetons squared, assuming an isotropic exchange interaction ($H = -2JS_1S_2$),

$$\mu_{\text{eff}}^2 = g_f^2 \sum_S \frac{S(S+1)(2S+1)\exp[-E(S)/k_BT]}{Z} \qquad (6)$$

where k_B is the Boltzmann factor, T is the temperature, $E(S) = -J_{ex}(\text{Fe–Fe})S(S+1)$, and $Z = \sum_S(2S+1)\exp[-E(S)/k_BT]$. At low temperatures (i.e. below 77 K), only the $S = 0$ and $S = 1$ states of the diferric center are significantly populated, and eq 6 can be simplified to eq 7. Equations 3, 5, and 7 predict

$$\mu_{\text{eff}}^2 = g_f^2\{6\exp[2J_{ex}(\text{Fe–Fe})/k_BT]\} \qquad (7)$$

that a plot of ln (k_{1ex}) or ln (k_{1d}) vs $1/T$ will have a slope of $2J_{ex}(\text{Fe–Fe})/k_B$.

Results

Identification of Spin–Lattice Relaxation Channels. The spin–lattice relaxation rates of the tyrosine radical of R2 ribonucleotide reductase from *E. coli*, HSV1, mouse, and *Salmonella* have been measured over 4 orders of magnitude by using saturation–recovery EPR spectroscopy. The observed recoveries for the four proteins are all single exponential in the low-temperature regime, $T < 10$ K; the spin–lattice relaxation rates below 10 K are also similar to those previously measured for a UV-generated tyrosine radical, which has been shown to be a good model for a noninteracting tyrosine radical.[3b,9] These observations indicate that the diferric center is diamagnetic at low temperature in all four proteins, due to antiferromagnetic exchange coupling of the two Fe(III) ions. As the temperature is increased, the tyrosine radicals in all four proteins show non-single-exponential recoveries with a marked increase in the temperature dependence of the relaxation rate. Figure 1 displays a saturation–recovery EPR transient from each R2 RNR at ~19 K. The dots are the data, and the superimposed solid line is the best fit of eq 1. From this fit, the scalar relaxation rate, $k_{1\text{scalar}}$, and the dipolar rate, k_{1d}, are extracted. The residuals from the fit are shown at the bottom of each transient.

Figure 2 displays the scalar component of the tyrosine radical's spin–lattice relaxation for HSV1, mouse, *E. coli*, and *Salmonella* R2 RNR. In the low-temperature regime, $T < 10$ K, the spin–lattice relaxation rates for the former three proteins are equivalent. As spin–phonon coupling is the mechanism of spin–lattice relaxation in this temperature region, it seems that the tyrosine radicals of these three species are accessing similar spin–phonon conversion pathways. However, the tyrosine radical in *Salmonella* R2 RNR relaxes approximately 5 times more slowly than the R2 RNR from the other species, for $T < 10$ K. In this low-temperature regime, the spin–lattice relaxation rates for *Salmonella* R2 RNR are equivalent to those of the dark-stable tyrosine radical, $Y_D^\bullet$, of photosystem II, which are shown in Figure 2 for comparison.

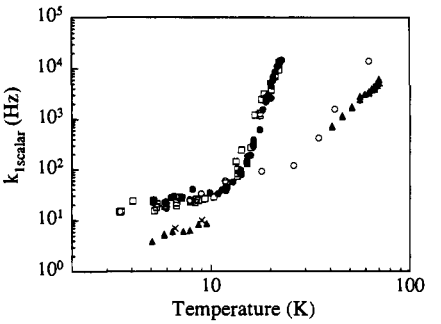

Figure 2. Temperature dependence of the scalar component ($k_{1\text{scalar}}$) of the spin–lattice relaxation of the tyrosine radicals in the R2 proteins from *E. coli* (○), HSV1 (□), mouse (●), and *Salmonella* (▲). Data for the dark-stable tyrosine radical, $Y_D^\bullet$, in photosystem II (×) are shown for comparison (taken from ref 16). The values of $k_{1\text{scalar}}$ were obtained by least-squares fits of eq 1 to saturation–recovery EPR transients taken at each temperature.

As the temperature increases, there is a dramatic diversion among the spin–lattice relaxation rates of HSV1, mouse, and *E. coli* R2 RNR. The temperature dependence of the relaxation rates increases sharply above approximately 15 K, indicating new relaxation channels available to the radical spin. It is in this temperature region that population of paramagnetic excited states of the diferric center begins to occur, and this results in new exchange and dipole–dipole coupling relaxation mechanisms. At 30 K, the scalar component of the spin–lattice relaxation rate of the tyrosine radical in the R2 proteins from HSV1 and mouse is approximately 2 orders of magnitude larger than that observed for the *E. coli* protein (Figure 2). These results are in good agreement with progressive microwave power saturation studies at the same temperature.[9,10]

The rate and temperature dependence of the spin–lattice relaxation also increased for the tyrosine radical in the *Salmonella* R2 protein in the high-temperature regime, although not as dramatically as observed in the other species. At 50 K, the spin–lattice relaxation of the tyrosine radical in the *Salmonella* R2 protein is 5 times slower than in the *E. coli* R2 protein and approximately 4 orders of magnitude slower than in the HSV1 and mouse R2 proteins.

Determination of the Diferric Exchange Coupling, J_{ex}(Fe–Fe). In the high-temperature regime, the spin–lattice relaxation of the tyrosine radical in the R2 protein is completely dominated by the exchange and dipolar mechanisms described by eqs 3 and 5, respectively. Consider, for example, the values of $k_{1\text{scalar}}$ plotted in Figure 2 for the HSV1 and mouse R2 proteins. Above about 20 K, the observed relaxation rates greatly exceed the expected intrinsic spin–lattice relaxation rates, based on an extrapolation of the low-temperature data to higher temperatures. Recalling eq 2 and in the limit where $k_{1\text{scalar}} \gg k_{1i}$, we conclude that $k_{1\text{scalar}} = k_{1ex}$ in the high-temperature regime.

There are two potentially temperature-dependent terms in the expressions for k_{1ex} and k_{1d}, eqs 3 and 5, respectively. The magnetic moment of the diferric center, μ_{eff}, will change with temperature as higher spin states are thermally populated. The spin–spin correlation time of the diferric center, T_{2f}, is also potentially temperature-dependent. However, T_{2f} is not expected to be temperature-dependent for an ensemble of noninteracting spins held in a rigid matrix such as a glass. Indeed, it was concluded that the value of T_{2f} of the diferric center in the *E. coli* R2 protein was not significantly temperature-dependent up to 77 K.[3b] When the temperature dependence of T_{2f} is negligible with respect to the temperature dependence of the magnetic moment of the diferric center, then the temperature dependence of the tyrosine radical's spin–lattice relaxation rate (eqs 3, 5, and 7) can be used to determine the diferric exchange coupling,

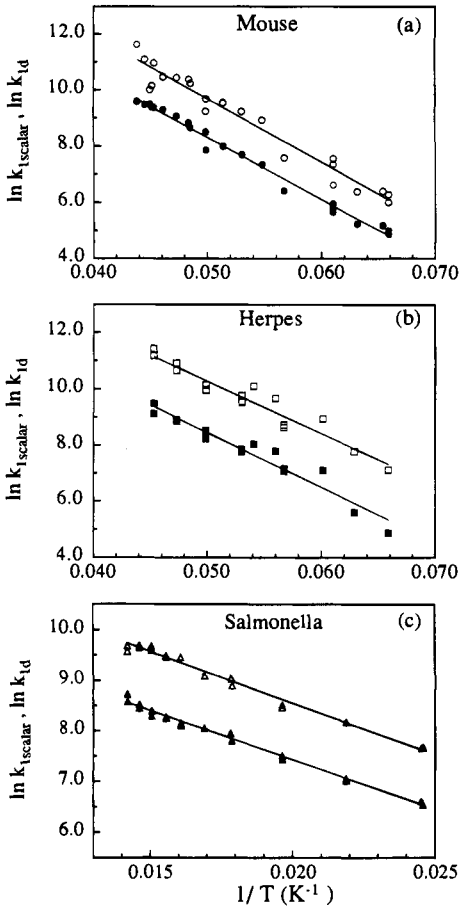

Figure 3. Plots of ln ($k_{1scalar}$) (solid symbols) and ln (k_{1d}) (open symbols) *vs* $1/T$ for data from the tyrosine radicals in the R2 proteins from (a) mouse, (b) HSV1, and (c) *Salmonella*. The values of $k_{1scalar}$ and k_{1d} were obtained by least-squares fits of eq 1 to saturation–recovery EPR transients taken at each temperature. In the high-temperature regime, the slopes of these plots yield J_{ex}(Fe–Fe), see eqs 3, 5, and 7 and text. The superimposed solid line is the best linear least-squares fit to the data, and the resulting values of J_{ex}(Fe–Fe) are given in Table 1.

Table 1. Exchange and Dipolar Interactions of the Diferric Center in the R2 Proteins

protein source	$-J_{ex}$(Fe–Fe) (cm^{-1})[a]	d_{Fe-O} (Å)[b]	$[(k_{1ex}/k_{1d})^{1/2}]$[c]
E. coli (data not shown)	92 ± 6	1.81	0.57 ± 0.05
herpes (HSV1)	66 ± 5	1.84	0.40 ± 0.06
mouse	77 ± 4	1.82	0.50 ± 0.04
Salmonella	69 ± 3	1.83	0.56 ± 0.04

[a] Determined from the slopes of the plots shown in Figure 3. [b] d_{Fe-O} is the iron–μ-oxo bond length calculated using the values of $-J_{ex}$(Fe–Fe) and the correlation of Gorun and Lippard.[20] [c] Calculated from the values obtained from least-squares fits of the data shown in Figure 3.

J_{ex}(Fe–Fe). This method was used to determine J_{ex}(Fe–Fe) = -94 ± 7 cm^{-1} in the *E. coli* R2 protein,[3b] which compares well with values of -108^{+25}_{-20} cm^{-1} and -84 ± 5 cm^{-1} determined by static magnetic susceptibility measurements.[3a,c]

Plots of ln $k_{1scalar}$ and ln k_{1d} vs $1/T$ are shown in Figure 3 for data from the tyrosine radicals in the R2 proteins from HSV1, mouse, and *Salmonella*. The slopes of the plots are, as expected, equivalent to within experimental error for a given species. Also, as expected from the divergence among species in the values of $k_{1scalar}$ depicted in Figure 2, $-J_{ex}$(Fe–Fe) for the HSV1 and mouse proteins is appreciably smaller than for the *E. coli* protein (Table 1). The value of J_{ex}(Fe–Fe) for the R2 protein from *E. coli* obtained previously (-94 ± 7 cm^{-1})[3b] was reproduced in the present study (-92 ± 6 cm^{-1}, data not shown). Quite unexpected was the finding of -69 ± 3 cm^{-1} for J_{ex}(Fe–Fe) in *Salmonella* R2 RNR, in which the tyrosine radical is more easily saturated by microwave power and could perhaps have been expected to have a much larger value of $-J_{ex}$(Fe–Fe). Thus, there is no straightforward relationship between the progressive microwave power saturation of the radical and the exchange coupling of the diferric center in these proteins. Also, structural differences have to be considered, as will be discussed below.

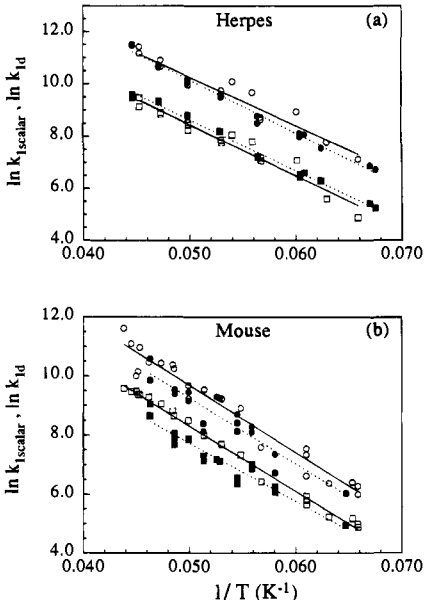

Figure 4. Effect of D_2O exchange on the temperature dependence of the scalar ($k_{1scalar}$, squares) and dipolar (k_{1d}, circles) components of the spin-lattice relaxation of the tyrosine radicals in the R2 proteins from (a) HSV1 and (b) mouse. The open symbols are the data from the proteins in natural media, and the filled symbols are the data from the proteins in deuterated media. The values of $k_{1scalar}$ and k_{1d} were obtained by least-squares fits of eq 1 to saturation–recovery EPR transients taken at each temperature. The superimposed lines are the best linear least-squares fits to the data: solid lines, natural media and dashed lines, deuterated media.

Determination of the Diferric Exchange Coupling for Proteins in Deuterated Buffer. In order to explore a possible role of hydrogen bonding to the μ-oxo bridge in the diferric exchange coupling, the tyrosine radical's spin–lattice relaxation was measured in the R2 proteins from HSV1 and mouse after reconstitution in deuterated buffer. Progressive microwave power saturation experiments at 25 K on the tyrosine radical in the R2 protein from HSV1 grown in deuterated media showed no difference from the natural media counterpart. The results of the saturation–recovery EPR investigation (Figure 4) show both the scalar and dipolar relaxation components in the deuterium-substituted sample to be the same, within the experimental error, as those from the sample in natural media.

The tyrosine radical in the R2 protein from mouse reconstituted in deuterated buffer, however, saturated at 25 K at about 0.5 the power required to saturate the tyrosine radical in the nondeuterated sample. As seen in Figure 4, the spin–lattice relaxation rates of the tyrosine radical in the deuterium-substituted sample are consistently lower than those of the nondeuterated sample. Analysis of the temperature dependence of the data in Figure 4 from the mouse R2 protein (eqs 3, 5, and 7) indicates that $-J_{ex}$(Fe–Fe) is about 3 cm^{-1} smaller in the deuterium-exchanged sample than in the nondeuterated sample. Although the difference in these two values is not outside the experimental error of the measurement, it is consistent with the difference of about a factor of 2 observed in the progressive microwave power saturation measurements.

Such a difference in the diferric exchange coupling would be predicted for a change in the hydrogen bonding interactions experienced by the μ-oxo bridge.

Distance and Exchange Interaction between the Tyrosine Radical and the Diferric Center. While the different temperature dependences of the spin−lattice relaxation rates observed for the tyrosine radical in the R2 proteins can be explained by variations in $J_{ex}(Fe-Fe)$, there are also differences in the magnitudes of the spin−lattice relaxation rates that arise from variations among the proteins in the distance between the tyrosine radical and the diferric center, r, and/or the exchange interaction between the tyrosine radical and the diferric center, $J_{ex}(Fe_2-Y)$. Rearrangement of eqs 3 and 5 yields an expression for $(k_{1ex}/k_{1d})^{1/2}$ (eq 8). Table 1 gives the values obtained for the

$$\sqrt{\frac{k_{1ex}}{k_{1d}}} = \frac{2r^3 J_{ex}(Fe_2-Y)}{\beta\gamma_s g_f} \tag{8}$$

ratio $(k_{1ex}/k_{1d})^{1/2}$ for the R2 RNR proteins. If one makes the reasonable assumption that the species-dependent variation in g_f is small compared to the observed range of $(k_{1ex}/k_{1d})^{1/2}$, then a difference in r and/or $J_{ex}(Fe_2-Y)$ is the source of the $(k_{1ex}/k_{1d})^{1/2}$ variation.

$J_{ex}(Fe_2-Y)$ depends on the spatial overlap of the electronic wave functions of the diferric center and the tyrosine radical. The value of this coupling may be determined within the present model by the rearrangement of eq 8 to give eq 9. Evaluation of

$$|J_{ex}(Fe_2-Y)| = \frac{\beta\gamma_s g_f^2}{2r^3}\sqrt{\frac{k_{1ex}}{k_{1d}}} \tag{9}$$

the expression given in eq 9 by using the distance of 8.3 Å between the center of the tyrosine ring to the midpoint between the two Fe(III) ions observed in the *E. coli* R2 protein crystal structure yields a value of 0.0047 ± 0.0003 cm^{-1} for $J_{ex}(Fe_2-Y)$ in the *E. coli* R2 protein.[3b] This value was reproduced in the present study.

The point dipole model used by Hirsh et al.[3b] to describe the magnetic interactions between the tyrosine spin and the diferric center spin may be extended by considering the spatial distribution of the electron spins responsible for the couplings. When the spin delocalization is large with respect to the interspin distance, the point dipole model may be inadequate to describe $J_{ex}(Fe_2-Y)$. Figure 5 depicts the atoms comprising the tyrosine radical and the iron center in the *E. coli* R2 protein. The letters adjacent to the atoms indicate their crystallographic labels. The dipolar coupling between the spins on the tyrosine ring and the diferric center may be modeled as distributed dipoles comprised of pairwise interactions of spin densities localized on the point atoms of the interacting groups. The spin density distribution of the tyrosine radical in the *E. coli* R2 protein has been determined by EPR spectroscopy[17a] and refined by ENDOR spectroscopy;[17b] the resulting values[17b] are indicated by the size of the filled circle on each atom in Figure 5. The diferric $S = 1$ spin state is expected to be isotropic over Fe1 and Fe2; therefore, a normalized spin density value of 0.5 is assigned to these atoms for the calculation. The spin density of atom i of the tyrosine radical, ϱ_i interacts with the spin density of the iron atom j of the diferric center, ϱ_j. These pairwise interactions are summed as in eq 10. Use of this spin-weighted interaction

$$\langle r^{-3}\rangle = \sum_{ij}\frac{\varrho_i\varrho_j}{r_{ij}^3} \tag{10}$$

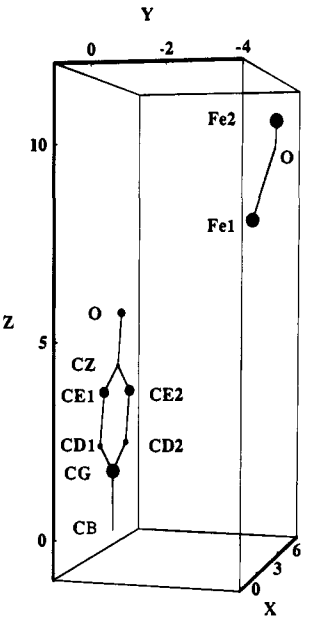

Figure 5. Structure[2] and spin distribution[17] of the *E. coli* R2 RNR tyrosine radical and diferric center. The atoms are labeled with the crystallographic labels, and the axes are in units of angstroms. The spin density values, shown by the size of the circles on each atom, were used in the calculations of the distributed dipole interaction between the tyrosine ring and the diferric center. In the cases of CD1, CD2, and CZ, the spin densities are negative. The coordinates[2] are taken from the known structure of the radical-free form of the R2 protein, which is assumed to be similar to the active protein with Tyr 122 in its radical form.

distance, $\langle r^{-3}\rangle$, in the evaluation of $J_{ex}(Fe_2-Y)$ yields 0.0068 cm^{-1}, an increase over the point dipole result of ~45%.

A consideration of the distributed dipole interactions suggests the possibility that a variation in the spin density distribution may be one source of the variation in $(k_{1ex}/k_{1d})^{1/2}$ among the different R2 proteins investigated. The static EPR spectra of the tyrosine radicals of the *E. coli*, HSV1, and mouse R2 proteins show sufficient similarity to suggest similar spin distributions over the tyrosine ring. On the other hand, it is possible that the distance and/or orientation of Tyr 122 with respect to the diferric center varies among the different R2 proteins. One possible structural variation among these proteins is the dihedral angle, ϕ, which describes the ring rotation about the bond CB−CG (see Figure 5). This dihedral angle determines the magnitude of the hyperfine coupling to the methylene protons adjacent to the tyrosine ring.[17] In order to investigate the impact of a variation of ϕ among species, $\langle r^{-3}\rangle$ was calculated as a function of ϕ over a 2π rotation of the tyrosine ring, by using eq 10 and assuming the structure and the spin densities on the tyrosine ring of the *E. coli* R2 protein shown in Figure 5. Because $(k_{1ex}/k_{1d})^{1/2}$ is proportional to r^3 (eq 8), we consider the variation of $(\langle r^{-3}\rangle)^{-1}$ with ϕ. $(\langle r^{-3}\rangle)^{-1}$ changed ~20%, occurring over a 120° range about the equilibrium value, ϕ_e. Rotation of the tyrosine ring about the CB−CG bond does not bring about larger changes in $(\langle r^{-3}\rangle)^{-1}$ mainly because the two large spin densities of the radical, 0.49 on CG and 0.16 on the tyrosine oxygen, lie on, or very nearly on, the axis of rotation. The effect of the remaining two large spin densities, 0.26 on both CE1 and CE2, is to somewhat cancel out the variation in ϕ. The quantity $(k_{1ex}/k_{1d})^{1/2}$ is also proportional to $J_{ex}(Fe_2-Y)$; however, this value cannot be calculated as a function of ϕ without large assumptions regarding the constituent molecular orbitals. Although the structural basis for the variation of $(k_{1ex}/k_{1d})^{1/2}$ among the four different R2 proteins remains to be determined, a change in the orientation of the

tyrosine ring relative to the diferric center could be sufficient to explain the variation. The static EPR spectrum of the tyrosine radical in the *Salmonella* R2 protein strongly resembles that of $Y_D^\bullet$ in photosystem II.[18] Since $Y_D^\bullet$ clearly differs from the tyrosine radical in the *E. coli* R2 protein in spin density distribution as well as dihedral angle,[19] it presents a special case in this comparison.

Discussion

We have confirmed the rapid spin−lattice relaxation of the tyrosine radical in the R2 proteins from HSV1 and mouse relative to that observed in the *E. coli* protein and have identified the primary source as a variation in the diferric exchange coupling, J_{ex}(Fe−Fe). The values determined for the diferric exchange for these three species are consistent with the observed spin-lattice relaxation rates. Such is not the case, however, for the spin−lattice relaxation rates of the tyrosine radical in the R2 protein from *S. typhimunium*, which, in the high-temperature regime, are on the order of 10−15 times slower than predicted by the diferric exchange coupling for this protein. In the low-temperature regime, as shown in Figure 2, the spin−lattice relaxation of the tyrosine radical in the R2 protein from *Salmonella* is appreciably lower than it is for the tyrosine radicals in the R2 proteins from other species. As mentioned above, the relaxation times of the tyrosine radical from *Salmonella* in this temperature regime are equivalent to those observed for the tyrosine radical, $Y_D^\bullet$, of photosystem II, which are plotted in Figure 2 for comparison. The static EPR spectra of the R2 proteins in the insets of Figure 1 show the *Salmonella* tyrosine radical to be quite unique with respect to the other protein radical spectra; the *Salmonella* R2 protein spectrum strongly resembles that of the $Y_D^\bullet$ of photosystem II.[18] As this spectrum is dominated by hyperfine interactions between the radical spin and the tyrosine ring protons, and the low-temperature regime relaxation rates of the *Salmonella* R2 RNR are equivalent to those of the $Y_D^\bullet$ of photosystem II, it seems likely that modulation of the hyperfine interaction is the dominant spin−lattice coupling mechanism.

In the high-temperature regime from $40 < T < 70$, the spin−lattice relaxation rates of the tyrosine radical in the *Salmonella* R2 protein are about 10−15 times slower than predicted by eqs 3 and 5, using the diferric exchange coupling for this species and the *E. coli* values for the remainder of the terms. There are a number of plausible explanations for the discrepancy. One factor is that the spin density distributions of the tyrosine radicals in the *E. coli* and *Salmonella* R2 proteins are different.[18,19] Even with the same spin distribution, the range of $(\langle r^{-3}\rangle)^{-1}$ as a function of tyrosine ring rotation was shown above to be sufficient to account for the observed range of $(k_{1ex}/k_{1d})^{1/2}$. However, a structural source for the slow spin-lattice relaxation of *Salmonella* R2 RNR would require a difference in tyrosine ring−diferric center orientation along some other degree of freedom, such as a ring bend or translation. Considering the unique local environment of the tyrosine radical in the *Salmonella* R2 protein indicated by the distinct static EPR spectrum, this is certainly possible. Another possibility is a difference among the proteins in the correlation time, T_{2f}, of the diferric center. It should also be noted that, as the spin-lattice relaxation times for the tyrosine radical in the *Salmonella* R2 protein in this temperature regime are not much greater than the relaxation times measured for UV-generated, isolated tyrosine radicals,[3b] the high-temperature assumption that $k_{1scalar} \gg k_{1i}$ may not be valid for this species.

Having analyzed the structural and magnetic properties of 36 (μ-oxo)diiron(III) complexes, Gorun and Lippard[20] proposed a correlation between the exchange interaction, J_{ex}(Fe−Fe), and the Fe−O distance (P), where P is the shortest exchange pathway between the two Fe(III) ions. Introducing the above J_{ex}(Fe−Fe) values into this relation leads to values of the Fe−O distance included in Table 1. It is important to note that these Fe−O distances are as expected for a (μ-oxo)(μ-carboxylato)-diiron entity. These distances seem to correlate with what is observed from EXAFS studies of proteins, although the Fe−O distance was reported to be 2.0 Å in the crystallographic structure of the *E. coli* R2 protein.[2] In methemerythrin ($-J_{ex}$(Fe−Fe) = 135 cm^{-1}) and azidomethemerythrin ($-J_{ex}$(Fe−Fe) calculated to be 142 cm^{-1}), the corresponding distances were reported as 1.80 and 1.76 Å, respectively.[21] Our observed variations in $-J_{ex}$(Fe−Fe) in the R2 proteins between 66 and 92 cm^{-1} could arise from small Fe−O distance variations between 1.84 and 1.81 Å, respectively.

Clearly, the present data on the R2 RNR proteins do not indicate the presence of a μ-OH bridge in any diferric R2 protein; a μ-OH-bridged diferric center would be expected to have a value of $-J_{ex}$(Fe−Fe) smaller than 17 cm^{-1}.[20]. For instance, the hydroxylase component of methane monooxygenase, with a demonstrated μ-OH bridge,[6] has $-J_{ex}$(Fe−Fe) = 7.5 cm^{-1}.[22] The decrease in $-J_{ex}$(Fe−Fe) from 135 cm^{-1} in hemerythrin to around 77 cm^{-1} in oxyhemerythrin has been suggested to result from an additional hydrogen bond to its μ-oxo bridge.[5c,20] We do not, at present, think that the HSV1 or mouse R2 proteins resemble oxyhemerythrin with respect to a bound O_2 molecule, but the presence of a weak hydrogen bond to the μ-oxo bridge cannot be excluded. The presence or absence of hydrogen bond interactions might be consistent with the changes in J_{ex}(Fe−Fe) observed between the species and the observed small effect of deuteration on the microwave power saturation properties. The use of other techniques is needed for a definitive answer. Such structural differences, although very subtle, could influence the redox properties of the iron centers. They might, therefore, also be related to the observation that it is easily possible to make mixed-valence forms of the mouse and HSV1 R2 proteins by mild chemical reduction, but not of the *E. coli* protein, which requires much more drastic methods.[23]

Acknowledgment. We wish to thank L. Thelander and R. Ingmarson, University of Umeå, P. Reichard, Karolinska Institute, and B.-M. Sjöberg, Stockholm University, for generous gifts of R2 proteins from mouse, herpes simplex virus type 1, *S. thyphimurium*, and *E. coli*, respectively, and A. Ehrenberg, Stockholm University, for reading the manuscript. This work was supported by grants from the National Institutes of Health (GM36442), the Bank of Sweden Tercentenary Foundation, the Swedish Natural Science Research Council, Magnus Bergvalls Stiftelse, and a travel grant from the Swedish Natural Science Research Council.

JA942764I

(18) Atta, M.; Barra, A.-L.; Andersson, K. K.; Allard, P.; Gräslund, A., manuscript in preparation.
(19) Hoganson, C. W.; Babcock, G. T. *Biochemistry* **1992**, *31*, 11874−11880.
(20) Gorun, S. M.; Lippard, S. J. *Inorg. Chem.* **1991**, *30*, 1625−1630.
(21) Stenkamp, R. E.; Sieker, L. C.; Jensen, L. H. *J. Am. Chem. Soc.* **1984**, *106*, 618−622.
(22) Fox, B. G.; Hendrich, M. P.; Surerus, K. K.; Andersson, K. K.; Froland, W. A.; Lipscomb, J. D.; Münck, E. *J. Am. Chem. Soc.* **1993**, *115*, 3688−3701.
(23) Atta, M.; Andersson, K. K.; Ingemarson, R.; Thelander, L.; Gräslund, A. *J. Am. Chem. Soc.* **1994**, *116*, 6429−6430.